

Measuring Molecular, Neutral Atomic, and Warm Ionized Galactic Gas Through X-Ray Absorption

John S. Arabadjis and Joel N. Bregman
 Dept. of Astronomy, University of Michigan
 Ann Arbor, MI 48109-1090
 jsa@astro.lsa.umich.edu, jrbregman@umich.edu

ABSTRACT

We study the column densities of neutral atomic, molecular, and warm ionized Galactic gas through their continuous absorption of extragalactic X-ray spectra at $|b| > 25^\circ$. For $N_{\text{H},21\text{cm}} < 5 \times 10^{20} \text{ cm}^{-2}$, there is an extremely tight relationship between $N_{\text{H},21\text{cm}}$ and the X-ray absorption column, $N_{\text{H},x}$, with a mean ratio along 26 lines of sight of $N_{\text{H},x}/N_{\text{H},21\text{cm}} = 0.972 \pm 0.022$. This is significantly less than the anticipated ratio of 1.23, which would occur if He were half He I and half He II in the warm ionized component. We suggest that the ionized component out of the plane is highly ionized, with He being mainly He II and He III. In the limiting case that H is entirely HI, we place an upper limit on the He abundance in the ISM of $\text{He}/\text{H} \leq 0.103$.

At column densities $N_{\text{H},x} > 5 \times 10^{20} \text{ cm}^{-2}$, which occurs at our lower latitudes, the X-ray absorption column $N_{\text{H},x}$ is nearly double $N_{\text{H},21\text{cm}}$. This excess column cannot be due to the warm ionized component, even if He were entirely He I, so it must be due to a molecular component. This result implies that for lines of sight out of the plane with $|b| \sim 30^\circ$, molecular gas is common and with a column density comparable to $N_{\text{H},21\text{cm}}$.

This work bears upon the far infrared background, since a warm ionized component, anticorrelated with $N_{\text{H},21\text{cm}}$, might produce such a background. Not only is such an anticorrelation absent, but if the dust is destroyed in the warm ionized gas, the far infrared background may be slightly larger than that deduced by Puget *et al.* (1996).

1. Introduction

The three primary mass components of the Galactic interstellar medium are molecular gas, neutral atomic gas, and warm ionized gas. Of these components, the only one whose mass can be measured directly from emission is the neutral atomic gas because the intensity

of the 21 cm line of HI is directly proportional to the HI column, barring opacity corrections, which are generally small for sight lines out of the Galactic plane. The mass of molecular gas is generally determined by measuring the intensity of the opaque CO(1→0) line and applying a correction factor to convert it to a H₂ column. The weakness in determining the molecular mass is that the correction factor is not a constant of nature, but can depend upon environment. For the other important constituent, the warm ionized gas, one generally obtains an emission measure (a dispersion measure is obtained toward some pulsars), so in general, a filling factor must be assumed in order to convert the emission measure to a column density. Additional information about the warm ionized gas is gained from pulsar dispersion measures, which provide electron column densities toward individual pulsars. Unfortunately, the dispersion measure contains no information about the ionization state of the gas. Due to the difficulties of obtaining the mass of the molecular and warm ionized components, it would be valuable if there were a simple independent approach to this issue. Fortunately, such an independent approach is provided by the absorption of X-rays.

Measurements of the X-ray absorption column provides a linear measure of the mass along the line of sight, whether it be molecular, neutral atomic, or warm ionized gas. The reason for this is that the X-ray absorption is mainly determined by the column density of He, which does not form compounds, or through inner shell absorption by metals, whose cross section is nearly independent of whether it is molecular, in dust, or free-floating. For neutral atomic conditions, the cross section is dominated by H and He at energies below 0.28 keV, with He accounting for about 70-75% of the absorption in the 0.1-0.28 keV band. Metal absorption begins to contribute in the 0.28-0.5 keV range, contributing about 17% of the total cross section due to the presence of C and N. Since carbon is used in some instrumental windows, such as on *ROSAT*, there is poor instrumental sensitivity in this region. At energies above the oxygen edge at 0.53 keV, the metals account for at least half of the absorption, a trend that continues to higher energies. The absorption by metals takes place with inner shell electrons, so the cross sections are largely independent of the structure of the valence electrons or the degree of ionization (for modest ionization). Furthermore, the cross section is nearly independent of the fraction of metals in grains, since the grains are transparent to X-rays.

Warm ionized gas has a total column density that is about one-third of the neutral hydrogen column (Reynolds 1989, 1991), and although hydrogen absorption is absent, helium is still a strong absorber since it is expected to be mainly He I or He II. The absorbing properties of He depend on its ionization state, with He II being a less effective absorber than He I. Assuming that helium is half He I and half He II (Domgörgen and Mathis 1994), the total absorption cross section is estimated to be about 60% that of the neutral gas near 0.2 keV. This leads to the expectation that absorption by warm ionized

gas should be evident in X-ray absorption measurements.

For lines of sight through total hydrogen columns of $3 \times 10^{20} \text{ cm}^{-2}$, which is typical of sight lines out of the Galactic plane, the X-ray absorption is mainly determined by the helium column. For total hydrogen columns of $1 \times 10^{21} \text{ cm}^{-2}$, such as occurs in sight lines through molecular clouds or at low Galactic latitudes ($|b| < 20^\circ$), the X-ray absorption is mainly determined by the metals, with oxygen being especially important. Consequently, with suitably chosen background sources, one can use X-ray absorption columns to study the structure of the ISM, the relative columns of the different phases, the He abundance, the metal abundance, and the conversion between the CO intensity and H_2 . This is the first of several investigations by us in which we examine the relative amounts of HI and HII as well as the He abundance in the Solar neighborhood. This work has an important bearing on the nature of the reported extragalactic far infrared background, since it helps to determine the amount of far infrared emission that could originate in warm ionized gas in the Galaxy.

This study is possible due to the ability to determine accurate X-ray absorption columns for comparison with accurate HI columns. The X-ray observations discussed here are obtained with the *ROSAT* Position Sensitive Proportional Counter (henceforth, PSPC), which is sensitive from 0.1-2.4 keV. Effectively, energies below 0.15 keV do not enter into the analysis because an HI column of only $5 \times 10^{19} \text{ cm}^{-2}$ reaches optical depth unity at 0.15 keV, and nearly all lines of sight out of the Galaxy are greater than $1 \times 10^{20} \text{ cm}^{-2}$. X-ray absorption columns can be determined from PSPC data with only a 5-10% uncertainty by using mono-temperature regions of galaxy clusters. HI columns are taken from the new survey by Hartmann and Burton (1997), which has an accuracy of 5% or less, as discussed below. In the following sections, we describe our assessment of the accuracy of the HI surveys (§2) and the approach needed to obtain the most accurate X-ray absorption columns (§3). We apply this to determine the amount of warm ionized gas in the Solar neighborhood, which leads to interesting constraints for the He abundance (§4, 5). Also, these results indicate that far infrared emission from dust in warm ionized gas cannot explain the far infrared residual, which is likely to be extragalactic in origin (§5).

2. The Accuracy of the HI Measurements

The determination of the total HI column out of the plane of the Galaxy has been determined in several surveys, two of which minimize the effects of sidelobe contamination: the Bell Labs survey (Stark *et al.* 1992) and the recent Dwingeloo survey (Hartmann and Burton 1997, henceforth HB). The Bell Lab survey employed a horn antenna that is nearly

free from sidelobe contamination but has only modest resolution ($2^\circ \times 3^\circ$) so that small-scale variations in the HI column are unresolved. The survey covered all declination regions north of -40° and with no gaps between the beams. The Dwingeloo survey has better resolution ($30'$) but it is a traditional dish design, so all observations needed to be corrected for contamination from stray radiation, usually by Galactic plane emission entering through the sidelobes. This survey observed all regions north of -30 degrees declination with a beam spacing of $30'$ and a beamsize of $36'$, so the sky is slightly undersampled. The Bell Labs survey has been used widely in the past for determinations of the absorption by the Galaxy, such as for soft X-ray observations. We have tried to assess whether the new Dwingeloo survey adds a substantial improvement in accuracy for the determination of the HI column density.

To access the accuracy of the two surveys along lines of sight out of the Galactic plane, we have sought to compare these surveys to more accurate measurements that are not part of an all-sky survey. Along these lines, an effort was made by Lockman and collaborators using the $140'$ telescope to determine N_{H} , corrected for sidelobe contamination, toward a variety of quasars being used in the HST absorption line key project (Elvis, Wilkes, and Lockman 1989; Lockman and Savage 1995). The $140'$ telescope has better resolution ($21'$) than either the Dwingeloo or Bell Labs telescopes and sidelobe contamination was corrected in a procedure that maps the Bell Labs main beam, so the correction is tied to the Bell Labs measurements. The N_{H} data from these three sources were compared for 60 lines of sight that are representative of the full range of Galactic latitude and longitude represented by the HB survey. Because these lines of sight were chosen to be out of the plane, only two lines of sight have $N_{\text{H}} > 1 \times 10^{21} \text{ cm}^{-2}$ and the central two quartiles are bounded by the N_{H} values 2.0×10^{20} and $3.8 \times 10^{20} \text{ cm}^{-2}$.

The internal accuracy of each survey has been estimated by a variety of tests. Lockman, Jahoda, and McCammon (1986) have examined the Bell Labs survey as it pertains to the region in directions of low HI column density, and they estimate that the uncertainty is $1 \times 10^{19} \text{ cm}^{-2}$ (1σ) when all sources of error are included. There are several sources of error that contribute to this figure: the accuracy of the absolute calibration of the Bell Labs data, about 2% (Kuntz and Danly 1992); baseline uncertainties, leading to errors of typically $2 \times 10^{18} \text{ cm}^{-2}$ (Lockman, Jahoda, and McCammon 1986); stray radiation from the far sidelobes give errors of about $1 - 5 \times 10^{18} \text{ cm}^{-2}$; and noise contributes an uncertainty of about $1 - 3 \times 10^{18} \text{ cm}^{-2}$. Toward the southern limit of the survey, sidelobe contamination issues become more difficult to correct and the accuracy is expected to be lower. Finally, in directions of higher column density, opacity corrections will become important, for which there is not simple correction, and molecular gas is likely to be present.

The uncertainties in the HB survey have been examined in detail, with considerable attention paid to the calibration, and the near and the far sidelobe stray radiation corrections (Hartmann and Burton 1997). Their accuracy is typically about $0.5 - 1 \times 10^{19}$ cm^{-2} , or about 3% of the signal for lines of sight out of the plane.

Another approach to estimating the uncertainties is by comparing the results of the different surveys in the directions observed by Lockman, Jahoda, and McCammon (1986; henceforth LJM). We find a smaller fractional differences between the LJM and HB surveys than between the Bell Labs survey and either LJM or HB. The fractional differences between the LJM and HB survey are not dependent upon the column density, although the most discrepant line of sight occurs at low N_{H} (Fig. 1). This particular line of sight is at the very southern limit of the HB survey, so the sidelobe correction may not be as accurate as at higher declinations. Of the next three greatest fractional differences, one is at a southern declination (-20°) and the other two are at high declination (70°). It is unclear to us whether this is of significance since other lines of sight at such declination values show small differences between the two surveys and these three points are only slightly deviant from a Gaussian distribution based upon the remainder of the population.

We examined whether the difference in N_{H} depended upon the distance from the center of the pointings of the HB survey (e.g., on the degree of the interpolation required between pointings). One expects a 3-4% error to be introduced for offsets of 10-20', based upon the structure function analysis toward low N_{H} regions (Lockman *et al.* 1986; also similar results occur if one uses the relatively high N_{H} region at $b = +6^\circ$; after Bregman, Kelson, and Ashe 1993). This error introduced by the offset is significantly smaller than the 7.8% rms and was not easily isolated in our sample, but is an effect that is probably present. In the comparison of the two surveys, a slight concern is that there is a weak anticorrelation between the fractional N_{H} difference and N_{H} (Fig. 1). Also there is a slight offset in the mean N_{H} between the two works, but it is only a 1.7σ effect.

One may assume that the absolute error in the HB and Lockman surveys are the same and that there is a 3-4% difference in N_{H} introduced by the need to interpolate in the HB survey. Under these assumptions, we find that the true uncertainty of a measurement point in each sample is 5.0%. The error in the HB measurements are probably closer to 3% (discussed in Hartmann and Burton 1997), with 5% being a conservative value.

The accuracy of determining N_{H} in a line of sight using the Bell Labs data can be estimated in the same fashion, although in this case, the result from the Bell Labs data can be compared to both the HB survey and the Lockman columns. The comparison between the Bell Labs data and the Lockman data should have the greatest internal consistency since Lockman anchors their measurements to the Bell Labs observations. The standard

deviation between the two sets of measurements is 9.5% and the mean offset is 0.031, a 2.5σ difference from zero. Most of the difference between the two measurements can be attributed to the variation within the rather large beam of the Crawford Hill telescope. In the comparison with the HB survey, the offset is 0.054, a 3.5σ difference and the standard deviation is 12%. This difference and standard deviation is larger than anticipated.

The typical angular scale over which our X-ray column densities are determined is about $12'$, a factor of three smaller than the $36'$ diameter beam of the Dwingeloo observations, and so we sought to characterize the magnitude of the expected emission fluctuations within the Dwingeloo beam with an independent method. This was accomplished by analyzing the power spectrum of the 21 cm emission. The spatial power spectrum of HI structure is obtained by squaring the Fourier transform of a 21 cm sky brightness map (e.g. Crovisier and Dickey 1983). The integral of the power spectrum, weighted by the square of the Fourier-transformed windowing function, results in a measure of the mean square emission contrast of the observed region (see, e.g., the discussion in Peebles 1993). Using the power spectrum obtained by Crovisier and Dickey (1983) for Arecibo observations of HI in the Galactic plane, we calculated an rms emission contrast of 7% using a FWHM= $30'$ Gaussian window, consistent with our previous estimate.

In summary, the HB survey provides the best measurements of N_{H} over most of the sky, and for directions out of the plane and where opacity effects are unimportant, the uncertainty in a measurement should be 5%, if not better. In the comparison between X-ray absorption columns and HI columns, we will concentrate on regions where $N_{\text{H}} < 3 \times 10^{20} \text{ cm}^{-2}$ and away from the southern limit of the HB survey.

3. Suitability of X-Ray Sources for Absorption Studies

The goal of this X-ray analysis is to obtain X-ray absorption column densities through the Galaxy with uncertainties near 10%, which is needed to distinguish between absorption by warm ionized gas and by neutral gas. To achieve this goal, we examined the accuracy to which absorption columns could be determined for three classes of extragalactic sources: active galactic nuclei; early-type galaxies, and galaxy clusters. The most common background sources are AGNs, but there were two problems in determining accurate column densities. First, the intrinsic underlying spectrum is not known and a power-law description may be inadequate. Second, and possibly more important is that many AGNs exhibit intrinsic absorption of their own, so separating this from absorption by the Galaxy is difficult. Our fits for the X-ray absorption column toward several AGNs led to a mean value of N_{H} that was about 10-20% above the 21 cm value of N_{H} , which is about the difference

expected by the absorption from warm ionized gas (see also Fiore *et al.* 1994). However, we could never be confident that this difference was not due the two problems stated above, so we searched for more suitable background sources.

We considered early-type galaxies as potential background sources since their spectrum can often be characterized by a single temperature thermal plasma. For this fit, one needs to assume that a single-temperature is an accurate model and a metallicity must be assumed or fit to the spectrum. Unfortunately, there is considerable debate as to the correct metallicity for these systems, and the value of the metallicity assumed has a direct influence on the value of N_{H} that one obtains from the X-ray fits. Furthermore, multiple temperature models are needed for at least some galaxies (e.g., NGC 4365, Fabbiano *et al.* 1994; Buote and Fabian 1998), and there is some concern about the accuracy of the thermal plasma models at temperatures of 0.1-1 keV (Bauer and Bregman 1996). Despite these problems, we examined the X-ray absorption columns toward 16 of the brightest X-ray emitting early-type galaxies. The uncertainty in these columns were too large to make these useful sources, and often, an extremely low X-ray absorption column was indicated (well below N_{H} from 21 cm observations), which is non-physical. This latter result could be understood if there is some X-ray emitting gas below the mean temperature, which would be expected from cooling flows. However, until we have adequate information to create accurate and well-understood cooling flow models for these galaxies, these sources are poor choices to obtain the X-ray absorbing columns in this study.

Galaxy clusters appear to be the most useful targets against which to determine the X-ray absorbing columns because there are regions in clusters that provide simple well-defined spectra. The spectrum of galaxy clusters may be complex in the center due to cooling flows, but this is confined to within the cooling radius, about 100-200 kpc, or 1-2' for a cluster at $z = 0.05$. Beyond the central region, clusters appear to be fairly isothermal until the very outer parts near 1-2 Mpc, although these outer regions have a low surface brightness. Consequently, the region beyond the cooling flow, but where the X-ray surface brightness is still high, is an ideal region in which to define a spectrum. The gas temperature is characteristic of the mean cluster temperature and the mean metallicity has been measured, both by independent instruments (Einstein, GINGA, and ASCA). The temperature of the cluster gas is typically 5 keV, so the spectrum is dominated by free-free radiation, with the line contribution coming primarily from He-like and H-like ions, which are the easiest and most reliable to model. Furthermore, uncertainties in the gas temperature and metallicity have little effect in the determination of the X-ray absorption column because the metals are only weak contributors and because there is practically no difference in the spectrum within the *ROSAT* PSPC band of a 5 keV spectrum compared to a 6 keV or 4 keV spectrum, which is typical of the temperature uncertainties for a cluster.

4. Cluster Selection and the Resulting X-ray Absorption Columns

The types of clusters that were selected for this study fulfill a variety of properties, based upon Galactic latitude and longitude, X-ray brightness, and whether basic parameters are known for the hot gas, such as temperature and metallicity. The X-ray brightness must be sufficient such that the spectrum in an annulus outside the center has enough counts to place tight constraints on spectral fits. In obtaining spectra, it is advantageous to determine the background in the same exposure as the cluster, so we avoided the nearby and large Virgo cluster. It is desirable for the X-ray temperature and metallicity to be known so that the fitted PSPC spectrum has the fewest possible free parameters. Finally, the emphasis of the study is on modest and low Galactic column densities, typically $< 5 \times 10^{20} \text{ cm}^{-2}$, because for higher columns, molecular gas starts to become more common and opacity corrections must be considered for the neutral hydrogen column. Given the desired cluster characteristics, we began the study by choosing clusters from the flux limited high galactic latitude sample of Henry and Arnaud (1991; $F_x(2\text{-}10 \text{ keV}) > 3 \times 10^{-11} \text{ erg cm}^{-2} \text{ s}^{-1}$, $|b| > 20^\circ$) with the addition of the clusters Hydra-A and A2163, which were later found to meet the criteria. This is a complete sample, which is not absolutely necessary for a study such as this, since the modest Galactic columns do not bias the hard flux from which the sample was chosen.

Each of the clusters that was studied (Table 1) was processed with both the current XSPEC (see Arnaud 1996 for a review) and PROS (e.g. Conroy *et al.* 1993) packages with standard techniques. Spatial and temporal variations in the instrument (*ROSAT* PSPC B or C; see, e.g., Briel, Burkert, and Pfeffermann 1989) were corrected for using the latest PCPICOR task in FTOOLS 4.0, before spectra were extracted using the most recent response matrices (for PSPC B gain 1-2 or PSPC C gain 1). The data were screened for periods of high background and a background-subtracted spectral energy distribution was produced in a pair of annuli that are usually 3-6' and 6-9', with point sources removed. Exceptions to this include A0665 (3-6', 9-12'), A2163 (2-4', 4-6'), A2256 (6-9', 9-15'), and A1656 and A2199 (two off-center circular regions), where we wished to avoid multiple point sources or galaxies, or modulate the number of counts. Each spectrum was fit with a single-temperature model whereby the metallicity and temperature are fixed, and taken from other sources (White, Jones, and Forman 1997; White *et al.* 1991). By fixing these parameters, there are only two remaining parameters in the spectral fit: the normalization and the absorption column.

The most recent absorption correction procedure available in XSPEC is based upon the work of Bałucińska-Church and McCammon (1992; in the routine VPHABS), who include autoionization corrections for He as well as a cross section that is different

from the absorption model of Morrison and McCammon (1983; in the routine WABS). However, recent work by Yan, Sadeghpour, and Dalgarno (1998), who calculate a more accurate He cross section, shows that the He cross section in the soft X-ray band given by Bałucińska-Church and McCammon (1992) is too great. Consequently, we wrote another absorption routine for use in XSPEC that incorporates the accurate He cross section of Yan *et al.* (1998). All of our fitting is performed with this higher accuracy absorption routine. For the purposes of this paper, one of the important parameters is found to be the He to H ratio, and we generally use the fairly standard value of 0.10 (e.g., Osterbrock, Tran, and Veilleux 1992), but we also consider a value of 0.09, which was deduced from observations of the Orion nebula by Baldwin *et al.* (1991).

A successful fit is one in which the best-fit has at least a 5% chance of occurrence based upon the χ^2 (e.g., for 187 degrees of freedom, the reduced $\chi^2 < 1.18$, or 1.26 for 1%). In a few clusters the number of counts in each channel was sufficiently large that errors in the PSPC calibration produce an artificially large contribution to the χ^2 . In those cases we replaced our central source annuli with regions at larger distance and lower flux, producing fits with acceptable χ^2 values. Spectral fits to A1795 and 2A0335 are shown in figures 2 and 3 to demonstrate the wide range in Galactic absorption. Uncertainties in the resulting X-ray absorption column are based upon the deviation from the best-fit, which is the usual procedure. We show confidence contours in the two fitting parameters for A1795 and 2A0335 in Figures 4 and 5. The resulting accuracy of the X-ray absorption column, expressed as $N_{\text{H,x}}$ is typically 5-10%, as seen in Table 2. We include the free electron column density of the Taylor and Cordes (1993) model for comparison therein. The X-ray and 21 cm HB columns are compared in Figure 6.

5. The Nature of Warm Ionized and Molecular Gas

There is an astonishing division in the nature of the X-ray absorption near $N_{\text{H,x}} = 5 \times 10^{20} \text{ cm}^{-2}$ (Fig. 6; Table 2). For X-ray absorption columns below that value, the neutral hydrogen column entirely accounts for the X-ray absorption. However, for larger X-ray columns, there must be a gaseous absorption component in addition to the neutral hydrogen. Because of this natural division, we will discuss the implications of the results in these two separate regimes. These results have important consequences for the nature of the thick warm ionized “Reynolds” layer in the Galaxy, for the nature of molecular gas, as well as for the determination of the extragalactic far infrared background.

5.1. Implications for the Galactic Warm Ionized Layer

As discussed above, the X-ray absorption column should reflect the contributions from molecular gas, neutral gas, and warm ionized gas (provided most of the He is either He I or He II). Consequently, it was surprising to find that for $N_{\text{H},x} < 5 \times 10^{20} \text{ cm}^{-2}$, there is little room for contributions from any component besides neutral atomic gas. In order to quantify this result, we introduce the quantity C , defined through the expression $N_{\text{H},x} = C \cdot N_{\text{H},21\text{cm}}$. For $N_{\text{H},x} < 5 \times 10^{20} \text{ cm}^{-2}$, $C = 0.972 \pm 0.022$ (this is the average; the error-weighted average is nearly identical). Our statistical tests indicate that there is no significant trend of C with column density and that the standard deviation for a single point is 11%. The uncertainty in $N_{\text{H},21\text{cm}}$ was estimated to be 5%, so most of the contribution to the standard deviation is inferred to lie with $N_{\text{H},x}$ (about 10%; this is slightly larger than the median error associated with the X-ray fits). When we include the uncertainty in $N_{\text{H},21\text{cm}}$ with the uncertainty in $N_{\text{H},x}$ from the spectral fit, there is only one point that lies more than 2.5 sigma below the average line: the outer region of the Coma cluster. This may reflect unresolved variation in $N_{\text{H},21\text{cm}}$ by radio telescopes or the difficulty of correcting for stray radio radiation at the lowest column density levels.

Our results indicate that, at the 99% confidence level, $C < 1.023$, which means that only 2.3% of the optical depth could be caused by some component other than neutral hydrogen. At these column densities, the amount of molecular hydrogen is found to be small (Savage *et al.* 1977) and would not be detectable as excess X-ray absorbing material. However, the warm ionized component of interstellar gas was expected to be detectable at somewhat greater levels.

Warm ionized gas has been studied most extensively by Reynolds (1989, 1991), who finds that in the Solar circle, the integrated HII column through the entire disk is $2.3 \times 10^{20} \text{ cm}^{-2}$, while the total HI column is $6.2 \times 10^{20} \text{ cm}^{-2}$. Therefore, the HI+HII column is 37% larger than the HI column alone. However, $N_{\text{H},x}$ is not 37% larger than $N_{\text{H},21\text{cm}}$ because the opacity is lower in the warm ionized gas. If $\text{HeII}/\text{He} = 0.5$ in the warm ionized gas (Domgörgen and Mathis 1994; see discussion by Snowden *et al.* 1994), the warm ionized gas has an effective cross section that is about 62% of neutral gas at about 1/4 keV. This leads to the prediction that $C = 1.23$, which is significantly above the value of C found from our data.

There are a few possible explanations for the difference between the anticipated and observed ratio of $N_{\text{H},x}/N_{\text{H},21\text{cm}}$. First, it is important to recognize that the studies of H α emission from diffuse gas relates to the emission measure and can be converted to a column density only after adopting a filling factor for the gas. The determination of the electron column density derives directly from the pulsar dispersion measure (Taylor and Cordes

1993), although a dispersion measure provides no information about the ionization state of the gas. By combining these two types of measurement, filling factors can be determined, upon assuming that the gas causing the dispersion measure and the H α emission are one and the same.

One possible explanation is that our sight lines happen to avoid most of the ionized halo gas that causes the pulsar dispersion measure. The ionized gas out of the plane has a scale height of about 1 kpc, so Taylor and Cordes (1993) quantify this distribution by measuring the dispersion measure toward pulsars in globular clusters and the scattering measure from AGNs. Based upon the observations of globular cluster pulsars, there do not appear to be frequent holes in the electron distribution, so it is unlikely that our 13 galaxy clusters lie in regions of low electron column densities.

Another possibility is that the warm ionized gas is more highly ionized than previously anticipated, thereby reducing the X-ray absorption cross section. Calculations of the ionization state of the warm ionized gas place the HeI/He fraction at about 50% (Domgörgen and Mathis 1994) and we arrive at a similar result (for the mean ISM ionizing spectrum and CLOUDY; Ferland 1996). As mentioned above, this results in $C = 1.23$, far above our upper limit of 1.023. The situation is only marginally improved if all of the He is singly ionized; in that case $C = 1.18$. In order to be consistent with our X-ray absorption measurements, He would have to be at least 87% HeIII. Lowering the value of He/H to 0.09 reduces the required ionization fraction by less than 1%.

A high degree of ionization could also explain the lack of recombination line radiation from He I $\lambda 5876$ (Reynolds and Tufté 1995). For gas in photoionization equilibrium, this would require at least an order of magnitude increase in the density of ionizing radiation than estimated to exist in the Galactic disk and would require that there be an additional source of ionization. Alternatively, the electrons may be associated with cooling gas in a galactic fountain, which would naturally have a high degree of ionization. In order for this gas not to exceed the disk pressure, the mean temperature of the cooling gas would need to be no greater than about 5×10^5 K.

Another factor that enters into this analysis is the value of the He/H ratio. We have used a He/H ratio of 0.10 for the above analysis, which is the common value used in X-ray astronomy and is comparable to the Solar value of 0.098. However, the value in the interstellar medium has been determined from the HII regions in the Orion nebula by two groups, who find ratios of 0.089 and 0.101, with the differences being attributed to details about the dust properties (Baldwin *et al.* 1991; Osterbrock *et al.* 1992). If this lower value is correct, then C increases by 0.07 to 1.046 (Fig. 8), and at the 99% confidence level, $C < 1.10$. This limit on C is reached if at least 45% of the He is He III, with the remainder

being He II.

We suggest that the most likely explanation for the low value of C is that the gas is more highly ionized than gas in a typical hot HII region. The gas may be hot galactic fountain gas at 10^5 - 10^6 K or cooler gas that is subject to a more intense ionizing radiation field than previously believed. For this explanation to be sensible, the $H\alpha$ emitting gas would not be cospatial with the dispersion measure gas. Consequently, the $H\alpha$ emission would need to originate from denser, lower filling factor material than assumed by Reynolds (1989, 1991).

In passing, we note that our observations can be used to set an upper limit to the He abundance in the ISM by requiring that the X-ray absorption column not be smaller than the 21 cm column (i.e., $C \geq 1$). If we demand that $C = 1$ ($N_{H,x} = N_{HI}$, and $N_{HII} = 0$) then, at the 99% confidence level, $He/H \leq 0.103$.

5.2. The Detection of Molecular Gas by X-Ray Observations

One of the striking results for our sample is that for $N_{H,x} > 6 \times 10^{20} \text{ cm}^{-2}$, the amount of X-ray absorbing material is substantially in excess of the measured atomic column. Seven clusters show this significant excess absorption, which requires an equivalent neutral atomic absorption that is comparable to the 21 cm HI column. This is over an order of magnitude greater than the amount expected from warm ionized gas in these directions (Taylor and Cordes 1993), even if all of the He were in the form of He I. Consequently, the only viable candidate for this excess absorption is molecular gas. In support of this suggestion, we note that the presence of this extra absorption occurs at the same column density where molecular gas can self-shield against ultraviolet photons (Federman, Glassgold, and Kwan 1979) as well as at the column above which H_2 becomes abundant, based on Copernicus ultraviolet absorption line observations toward stars (Savage *et al.* 1977).

In order to extract the molecular column density from these measurements, we correct for the small opacity in the 21 cm line (3% effect) and for the slight increase in the X-ray opacity because H_2 has a cross section that is 40% larger, per H atom than HI (Yan, Sadeghpour, and Dalgarno 1998). At these column densities, about half of the opacity is due to H_2 and He (with He being the dominant of the two) with the remainder due to O, C, and N (O is the dominant metal absorber). We assume Solar abundances for the metals and that the X-ray absorption cross section for the metals is independent of whether they are in molecular or atomic form. The resulting fractional H_2 column is compared to the total inferred column of atoms, $N(HI+2H_2)$ (Fig. 9), similar to the approach taken by Savage *et*

al. (1977), whose results from ultraviolet H₂ studies are also shown. Our primary result is that for sightlines out of the disk where $N_{\text{H,x}} > 6 \times 10^{20} \text{ cm}^{-2}$, the amounts of atomic and molecular hydrogen are comparable. Our mean molecular fraction is about twice that of Savage *et al.*, for the same range of total atomic columns.

There are a few important differences in the location and distance of targets between our sample and that of Savage *et al.* Six of the seven clusters lie in the range $26^\circ < |b| < 40^\circ$ (the seventh lies at $b = -50^\circ$) and the sight lines sample the entire vertical extent of the disk. In the Savage *et al.* sample, all of the stars more distant than 0.5 kpc lie either at very low latitude in the plane, or at fairly high latitude where $N(\text{H}_2)$ is quite low. There are no distant stars at $|b| = 25 - 40^\circ$, and our sample has no clusters at $|b| < 25^\circ$. Our work samples the atomic and molecular gas in the Solar neighborhood at mid-latitudes, while the Savage *et al.* work primarily samples sight lines through the disk and this difference in sampling may be responsible for the slightly different molecular gas fractions. Also, the stars in Savage *et al.* are hot stars, which may be able to destroy local molecular gas, thereby decreasing the molecular fraction, an effect that would be greatest for the nearest stars.

Another investigation that our work can be compared to is the study of HCO⁺ and OH absorption toward extragalactic sight lines (Lucas and Liszt 1996 and references therein). At Galactic latitudes below 39° , 18 of 22 sightlines were detected as HCO⁺ absorbers, indicating that molecular gas is quite common. They must adopt a conversion of $N(\text{HCO}^+)$ to $N(\text{H}_2)$, so there is greater uncertainty than the direct measurement of H₂ by Savage *et al.* (1977). Nevertheless, their molecular hydrogen columns are similar to those of Savage *et al.* (1977), and slightly lower than our molecular fractions. Attempts to measure this H₂ gas by CO surveys at moderate and high galactic latitudes fail to detect abundant CO emission (Hartmann, Magnani, and Thaddeus 1998), a result that must reflect the fact that CO is destroyed before H₂. Finally, we note that molecular gas may be a considerable if not dominant fraction of the gas mass in the outer part of the Milky Way according to Lequeux, Allen, and Guilleaume (1993).

The presence of molecular gas is reflected in the far infrared emission as observed by the *IRAS* satellite. We extracted the *IRAS* 100 μm observations in the direction of each of the clusters, as shown in Figure 7. Each of the lines of sight whose column density $N_{\text{H},21\text{cm}} > 5 \times 10^{20} \text{ cm}^{-2}$ (i.e. the filled circles in Fig. 6) shows moderate or substantial structure in its 100 μm emission. For example, 2A0335 lies behind a large tongue of far infrared *IRAS* emission and its position is adjacent to a known molecular cloud. It is possible that molecular gas, just below the threshold of the instrument, lies in front of 2A0335.

Earlier, we considered the possibility that fluctuations in the HI distribution might lead us to infer 21 cm columns that were inaccurate, but the analysis of 21 cm data indicated that the uncertainties would be at the 5% level in N_{HI} . This test can also be conducted by examining the fluctuations in the total gas column as reflected in the *IRAS* 100 μm fluxes. In particular, we examine whether there might exist large column density fluctuations within the 36' diameter beam of the HI survey. The most direct method of making this test is to compare the $F_\nu(100\mu\text{m})$ within the annuli used for the X-ray measurements with the $F_\nu(100\mu\text{m})$ within a 36' diameter region. Using 100 μm images centered on the clusters, we divided each image into 6 concentric annuli, each with a thickness of 3'. We calculated the 100 μm flux averaged over each annulus (i.e. the differential mean) and also over the entire disk contained within each annulus (the cumulative mean; Fig. 10). In each case we calculated the relative difference δf_ν between $F_\nu(100\mu\text{m})$ averaged over the 36' (diameter) disk and $F_\nu(100\mu\text{m})$ averaged over the 6-12' annulus, corresponding to the HB beam and the X-ray absorption calculations, respectively. The mean value of $|\delta f_\nu|$ for the seven clusters is 5%, and the mean value of δf_ν is -0.3%, indicating that the errors in $F_\nu(100\mu\text{m})$ are consistent with being random at the 5% level. This is the same degree of fluctuation found from the HI analysis.

The 100 μm flux is known to correlate with HI gas, although nonlinearly and with significant scatter (e.g., Boulanger *et al.* 1996). Here we examine whether the correlation is modified when correlating the X-ray absorption column with the far infrared emission. We obtained values for the 100 μm fluxes from the public *IRAS* products (using IRSKY 2.3.1), in which the Zodiacal light contribution has been removed with a model, although this is not the latest model (Shafer *et al.* 1997). A least-squares fit between N_{HI} and $F_\nu(100\mu\text{m})$ yields $N_{\text{HI}} \propto F_\nu(100\mu\text{m})^{0.57 \pm 0.29}$. The departure of the exponent from unity was thought to be due in part to the inability to include $N(\text{H}_2)$ along the line of sight, and to the oversubtraction of the estimated Zodiacal flux at low levels.

Improved determinations of the far infrared fluxes are available through the recent work of Schlegel *et al.* (1998), who have reprocessed the *IRAS* data together with the *COBE/DIRBE* maps. Relative to the older standard *IRAS* products, these values for $F_\nu(100\mu\text{m})$ are often significantly different at low flux levels, generally being larger. This leads to steeper relationships, with $N_{\text{HI}} \propto F_\nu(100\mu\text{m})^{0.84 \pm 0.27}$ and $N_{\text{H,x}} \propto F_\nu(100\mu\text{m})^{1.16 \pm 0.22}$ (Fig. 11), consistent with unity.

6. Implications for the Far Infrared Background

These results have an important consequence for the intensity of the far infrared background (Puget *et al.* 1996; Boulanger *et al.* 1996) because those investigators needed to remove the Galactic far infrared signal associated with the neutral and ionized gas around the Sun. After correcting for Zodiacal emission and the 3 K background, they remove a Galactic far infrared signal that is proportional to the HI column, resulting in a positive residual. This is the only correction to Galactic gas if the relative columns of neutral and warm ionized gas are constant and if the dust temperature in these regions is independent of the column density. However, there is the concern that this ratio of the neutral to warm ionized column densities is not a constant and that the warm ionized column increases as N_{HI} decreases. These investigators consider that possibility and subtract an additional far infrared signal that is due to an additional column density of ionized gas of amount $4 \times 10^{19} \text{ cm}^{-2}$. In comparison, Schlegel *et al.* (1998) and Shafer *et al.* (1997) also find evidence for a far infrared background above $100\mu\text{m}$, although they do not explicitly remove a separate column density of warm ionized gas.

Based upon our X-ray absorption measurements, there is no evidence for an inverse correlation between the neutral and warm ionized gas. As shown above, for $N_{\text{HI}} < 5 \times 10^{20} \text{ cm}^{-2}$, there is little room for warm ionized gas of moderate ionization state, although we know that ionized material is present at about the level assumed by Puget *et al.* (1996) based upon the pulsar dispersion measurements. If the dust is destroyed in this ionized material, as might occur if the gas had been heated to $\sim 10^6 \text{ K}$, as in a galactic fountain picture, then Puget *et al.* (1996) have subtracted too much far infrared emission, and the far infrared background is somewhat brighter than they calculated. However, if the dust is not destroyed in this ionized column, and if it is at the mean temperature of dust nearer the disk, then they have dealt with this contribution correctly, in which case the far infrared background as determined by Shafer *et al.* (1997) may be too high.

We have examined the utility of using the X-ray columns and the $F_{\nu}(100\mu\text{m})$ of Schlegel *et al.* (1998) to examine the presence of the far infrared background. When we perform a linear fit of $F_{\nu}(100\mu\text{m})$ on N_{HI} , we find that when $N_{\text{HI}} = 0$, $F_{\nu}(100\mu\text{m}) = 0.04 \pm 0.31$ (Fig. 12), which is indistinguishable from zero, as Schlegel *et al.* (1998) found, for a larger data set. However, when we compare the X-ray column to the far infrared flux, we obtain a background $F_{\nu}(100\mu\text{m}) = 0.26 \pm 0.10 \text{ MJy sr}^{-1}$ (Fig. 13), which is slightly larger but consistent with the value of Puget *et al.* (1996), 0.12 MJy sr^{-1} . We do not claim that our work shows a convincing detection of the far infrared background, since it is not even a 3σ result. However, we hope that this demonstrates the feasibility of the approach and we note that the sample can be expanded substantially, probably to 100-200 clusters, which would

reduce the uncertainty. Also, future instruments will have better spectral capabilities, which will improve the accuracy of individual measurements of $N_{\text{H},x}$.

We would like to give special thanks to F.J. Lockman and D. Hartmann for their responses and guidance to the many questions that we raised. Also, we would like to thank X. Desert, J.P. Puget, Eli Dwek, Bill Reach, S. Snowden, D. McCammon, K. Arnaud, C. McKee, J. Cordes, S. Spangler, R. Lucas, S. Tufte, R. Reynolds, M. Bremer, and G. Mamon for stimulating conversations on this topic. JNB would like to thank A. Omont as well as the faculty and staff at the Institut d’Astrophysique for their hospitality during which this work was begun. This work made extensive use of the *ROSAT* data archive facility at the HEASARC as well as the NASA Extragalactic Database. Archived infrared data were obtained with IRSKY 2.3.1 and the FITS interface and maps of D. Schlegel, D. Finkbeiner, and M. Davis. Financial support for this work was provided for by NASA grants NAG5-3247 and NAG5-3352.

REFERENCES

- Arnaud, K.A. 1996, *Astron. Soc. Pac. Conf. Ser.*, **101**, 17.
- Baldwin, J.A., Ferland, G.J., Martin, P.G., Corbin, M.R., Cota, S.A., Peterson, B.M., and Slettebak, A. 1991, *Ap. J.*, **374**, 580.
- Bałucińska-Church, M., and McCammon, D. 1992, *Ap. J.*, **400**, 699.
- Bauer, F., and Bregman, J.N. 1996, *Ap. J.*, **457**, 382.
- Boulanger, F., Abergel, A., Bernard, J.-P., Burton, W.B., Desert, F.-X., Hartmann, D., Lagache, G., and Puget, J.L. 1996, *Astron. Astrophys.*, **312**, 256.
- Bregman, J.N., Kelson, D.D., and Ashe, G.A. 1993, *Ap. J.*, **409**, 682.
- Briel, U.G., Burkert, W., and Pfeffermann, E. 1989, *X-ray Calibration of the ROSAT Position-sensitive Proportional Counter: the Energy Calibration*, in *EUV, X-Ray, and Gamma-Ray Instrumentation for Astronomy and Atomic Physics*, Charles J. Hailey and Oswald H. Siegmund, Eds., *Proc. SPIE*, **1159**, 263.
- Buote, D.A., and Canizares, C.R. 1998, *M. N. R. A. S.*, in press; also astro-ph/9707117.
- Conroy, M.A., DePonte, J., Moran, J.F., Orszak, J.S., Roberts, W.P., and Schmidt, D. 1993, *Astron. Soc. Pac. Conf. Ser.*, **52**, 238.
- Crovisier, J., and Dickey, M. 1983, *Astron. Astrophys.*, **122**, 282.
- Domgörgen, H., and Mathis, J.S. 1994, *Ap. J.*, **428**, 647.
- Elvis, M., Wilkes, B.J., and Lockman, F.J. 1989, *Astron. J.*, **97**, 777.
- Fabbiano, G., Kim, D.-W., and Trinchieri, G. 1994, *Ap. J.*, **429**, 94.
- Federman, S.R., Glassgold, A.E., and Kwan, J. 1979, *Ap. J.*, **227**, 466.
- Ferland, G.J. 1996, *A Brief Introduction to CLOUDY*, Univ. of Kentucky Dept. of Physics and Astronomy Internal Report.
- Fiore, F., Elvis, M., McDowell, J.C., Siemiginowska, A., and Wilkes, B.J. 1994, *Ap. J.*, **431**, 515.
- Hartmann, D., and Burton, W.B. 1997, *Atlas of Galactic Neutral Hydrogen*, Cambridge University Press.
- Hartmann, D., Magnani, L., and Thaddeus, P. 1998, *Ap. J.*, **492**, 205.
- Henry, J.P., and Arnaud, K.A. 1991, *Ap. J.*, **372**, 410.
- Lequeux, J., Allen, R.J., and Guilloteau, S. 1993, *Astron. Astrophys.*, **280**, L23.
- Lockman, F.J., and Savage, B.D. 1995, *Ap. J. Supp. Ser.*, **97**, 1.

- Lockman, F.J., Jahoda, K., and McCammon, D. 1986, *Ap. J.*, **302**, 432.
- Lucas, R., and Liszt, H. 1996, *Astron. Astrophys.*, **307**, 237.
- Morrison, R., and McCammon, D. 1983, *Ap. J.*, **270**, 119.
- Osterbrock, D.E., Tran, H.D., and Veilleux, S. 1992, *Ap. J.*, **389**, 305.
- Peebles, P.J.E. 1993, *Principles of Physical Cosmology*, Princeton University Press.
- Puget, J.-L., Abergel, A., Bernard, J.-P., Boulanger, F., Burton, W.B., Desert, F.-X., and Hartmann, D. 1996, *Astron. Astrophys.*, **308**, L5.
- Reynolds, R.J. 1989, *Ap. J.*, **339**, L29.
- Reynolds, R.J. 1991, *Ap. J.*, **372**, L17.
- Reynolds, R.J., Tufte, S.L. 1995, *Ap. J.*, **439**, L17.
- Savage, B.D., Bohlin, R.C., Drake, J.F., and Budich, W. 1977, *Ap. J.*, **216**, 291.
- Schlegel, D.J., Finkbeiner, D.P., and Davis, M. 1998, *Ap. J.*, in press.
- Shafer, R.A., Mather, J.C., Fixsen, D.J., Brodd, K., and Jensen S.A. 1997, *Bull. Amer. Ast. Soc.*, **191**, 96.06.
- Snowden, S.L., Hasinger, G., Jahoda, K., Lockman, F.J., McCammon, D., and Sanders, W.T. 1994, *Ap. J.*, **430**, 601.
- Stark, A.A., Gammie, C.F., Wilson, R.W., Bally, J., Linke, R.A., Heiles, C., and Hurwitz, M. 1992, *Ap. J. Supp. Ser.*, **79**, 77.
- Taylor, J.H., and Cordes, J.M. 1993, *Ap. J.*, **411**, 674.
- White, D.A., Jones, C., and Forman, W. 1997, *M. N. R. A. S.*, **292**, 419.
- White, D.A., Fabian, A.C., Johnstone, R.M., Mushotzky, R.F., and Arnaud, K.A. 1991, *M. N. R. A. S.*, **252**, 72.
- Yan, M., Sadeghpour, H.R., and Dalgarno, A. 1998, *Ap. J.*, **496**, 1044.

Table 1. The cluster sample.

cluster	l^I	b^I	T ^a , keV	z^a
2A0335	176.25	−35.08	3.1	0.035
A0085	115.05	−72.08	6.2	0.0521
A0119	125.75	−64.11	5.1	0.0443
A0133	149.09	−84.09	3.8	0.0604
A0401	164.18	−38.87	7.8	0.0748
A0478	182.43	−28.29	6.8	0.0881
A0496	209.59	−36.49	4.7	0.0330
A0665	149.73	+34.67	8.3	0.1816
A1060	269.63	+26.51	3.3	0.0124
A1651	306.83	+58.62	7.0	0.0825
A1656	58.16	+88.01	8.0	0.0231
A1795	33.81	+77.18	5.1	0.0621
A2029	6.49	+50.55	7.8	0.0765
A2052	9.42	+50.12	3.4	0.0348
A2142	44.23	+48.69	11.0	0.0899
A2147	28.83	+44.50	4.4	0.0356
A2163	6.75	+30.52	13.9	0.2030
A2199	62.93	+43.69	4.7	0.0299
A2256	111.10	+31.74	7.5	0.0581
A2657	96.65	−50.30	3.4	0.0414

^aT, z from White, Jones and Forman (1997) and references therein, except for 2A0335, which is from White *et al.* (1991).

Table 2. Column densities toward each cluster in the sample (in units of 10^{20} cm^{-2}).

cluster	$N_{\text{H},x}(1)$ ^a	$N_{\text{H},x}(2)$ ^a	$N_{\text{H},21\text{cm}}$ ^b	N_e ^c
2A0335	27.8 ± 1.1	26.1 ± 1.7	17.4	0.855
A0085	2.78 ± 0.07	2.79 ± 0.10	2.89	0.534
A0119	3.35 ± 0.20	3.10 ± 0.18	3.45	0.562
A0133	1.46 ± 0.06	1.29 ± 0.09	1.60	0.512
A0401	12.6 ± 1.0	15.3 ± 1.7	9.57	0.787
A0478	33.9 ± 0.9	37.4 ± 1.5	14.1	1.02
A0496	7.02 ± 0.34	7.13 ± 0.52	4.11	0.830
A0665	4.73 ± 0.24	4.49 ± 0.88	4.24	0.867
A1060	6.75 ± 0.41	6.71 ± 0.33	4.87	1.15
A1651	1.59 ± 0.08	1.25 ± 0.11	1.47	0.602
A1656	0.781 ± 0.050	0.597 ± 0.071	0.90	0.509
A1795	0.909 ± 0.026	0.909 ± 0.017	1.04	0.525
A2029	3.23 ± 0.08	3.23 ± 0.13	3.18	0.673
A2052	3.10 ± 0.13	2.70 ± 0.18	2.71	0.676
A2142	4.17 ± 0.14	3.88 ± 0.21	3.86	0.688
A2147	2.52 ± 0.65	2.56 ± 1.12	2.82	0.741
A2163	22.4 ± 1.6	26.4 ± 2.5	11.0	1.05
A2199	0.830 ± 0.035	0.877 ± 0.047	0.81	0.744
A2256	4.47 ± 0.14	4.65 ± 0.13	4.16	0.950
A2657	11.3 ± 0.8	14.5 ± 1.4	6.00	0.660

^a $N_{\text{H},x}$ toward two different source regions in each cluster.

^b $N_{\text{H},21\text{cm}}$ from Hartmann and Burton (1997).

^c N_e calculated from the model of Taylor and Cordes (1993).

Figure captions

Fig_LS.ps

Fig. 1.— The fractional difference between the HI column densities of Hartmann and Burton (1997) compared to those of Lockman and collaborators (Elvis, Wilkes and Lockman 1989; Lockman and Savage 1995) where the abscissa is N_{HI} from Hartmann and Burton (1997). The lines of sight are toward active galactic nuclei, and the fractional difference is $(N(\text{Hartmann-Burton}) - N(\text{Lockman})) / N(\text{Lockman})$.

Fig_A1795fit.ps

Fig. 2.— A spectral fit to A1795, a low-absorption column cluster. The top panel shows the model spectrum convolved with the PSPC instrument response; the residuals are shown at the bottom.

Fig_2A0335fit.ps

Fig. 3.— A spectral fit to 2A0335, a large-absorption column cluster. The quantities shown are the same as in Fig. 2.

Fig_A1795con.ps

Fig. 4.— $\Delta\chi$ -square contours in normalization vs. $N_{\text{H,x}}$ for A1795. Moving outward, the contours have values of 2.3, 4.6, and 9.2, corresponding to confidence limits of 68%, 90%, and 99%.

Fig_2A0335con.ps

Fig. 5.— $\Delta\chi$ -square contours in normalization vs. $N_{\text{H,x}}$ for 2A0335. The contours have the same values as those in Fig. 4.

Fig_NHxNH.ps

Fig. 6.— The ratio of X-ray column density to the 21 cm column of Hartmann and Burton (1997). The lines of sight are toward the 20 sample clusters. The open circles represent directions of low column density which are used to estimate a fiducial $N_{\text{H,x}}/N_{\text{H,21cm}}$.

Fig_IRAS1.jpg

Fig_IRAS2.jpg

Fig. 7.— *IRAS* 100 μ m images toward each of the clusters in the sample. Each frame is 7.5° on a side, and the location of the cluster is indicated with a 40' diameter circle.

Fig_HHe.ps

Fig. 8.— A comparison of X-ray column densities for the low column density sight lines for two values of He/H. The error bars do not include uncertainties in N_{H} .

Fig_H2frac.ps

Fig. 9.— The fractional H₂ column as a function of the total inferred H column $N(\text{HI}+\text{H}_2)$. The triangles represent H₂ fractions derived by Savage *et al.* (1977) from ultraviolet absorption of molecular hydrogen.

Fig_ann.gif

Fig. 10.— Differential (dotted) and cumulative (solid) averages of the *IRAS* 100 μ m flux in the direction of the seven high-column clusters. The quantity δf_{ν} is defined as the relative difference between $\langle F_{\nu}(100\mu\text{m}) \rangle$ averaged over the entire 36' wide disk and $\langle F_{\nu}(100\mu\text{m}) \rangle$ averaged over the 6-12' annulus, corresponding to the HB beam and a fiducial X-ray column measurement.

Fig_NHF100.gif

Fig. 11.— Hydrogen column density determined from X-ray absorption (A) and from 21 cm emission (B; Hartmann and Burton 1997) versus *IRAS/DIRBE* 100 μ m flux (Schlegel *et al.* 1998) for the 20 clusters in the sample.

Fig_IR21.ps

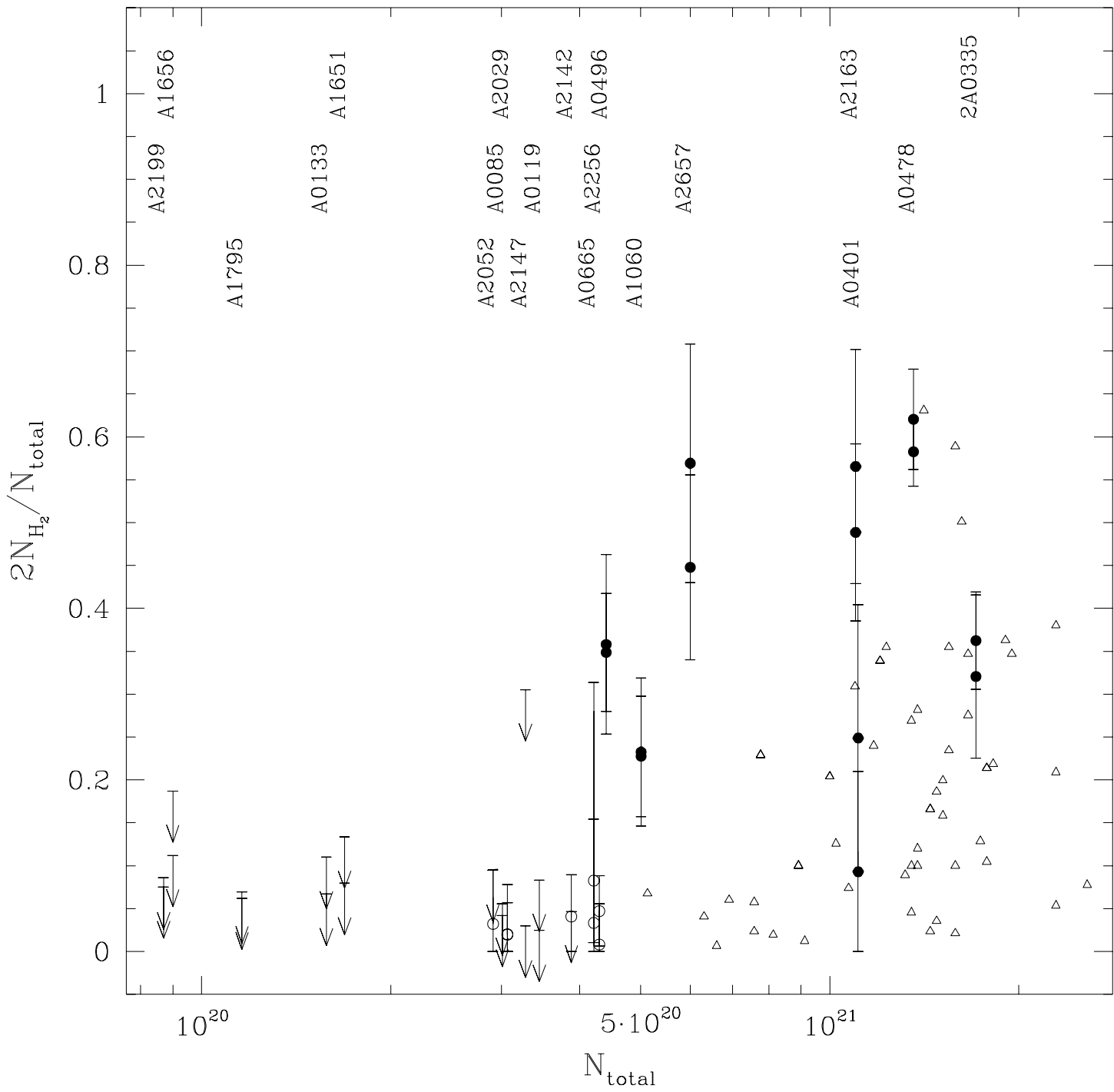
Fig. 12.— 21 cm column (Hartmann and Burton 1997) versus *IRAS/DIRBE* 100 μ m flux (Schlegel *et al.* 1998) for the 13 low-column clusters in the sample. At $N_{\text{HI}} = 0$, the 100 μ m flux is 0.04 ± 0.31 MJy sr⁻¹, consistent with zero.

Fig_IRX.ps

Fig. 13.— X-ray absorption column versus *IRAS/DIRBE* 100 μm flux (Schlegel *et al.* 1998) for the 20 clusters in the sample. At $N_{\text{HI}} = 0$, the 100 μm flux is $0.26 \pm 0.10 \text{ MJy sr}^{-1}$. If we use only the 13 low-column clusters, this flux becomes $0.22 \pm 0.24 \text{ MJy sr}^{-1}$. The inset is an enlargement of the region near the origin.

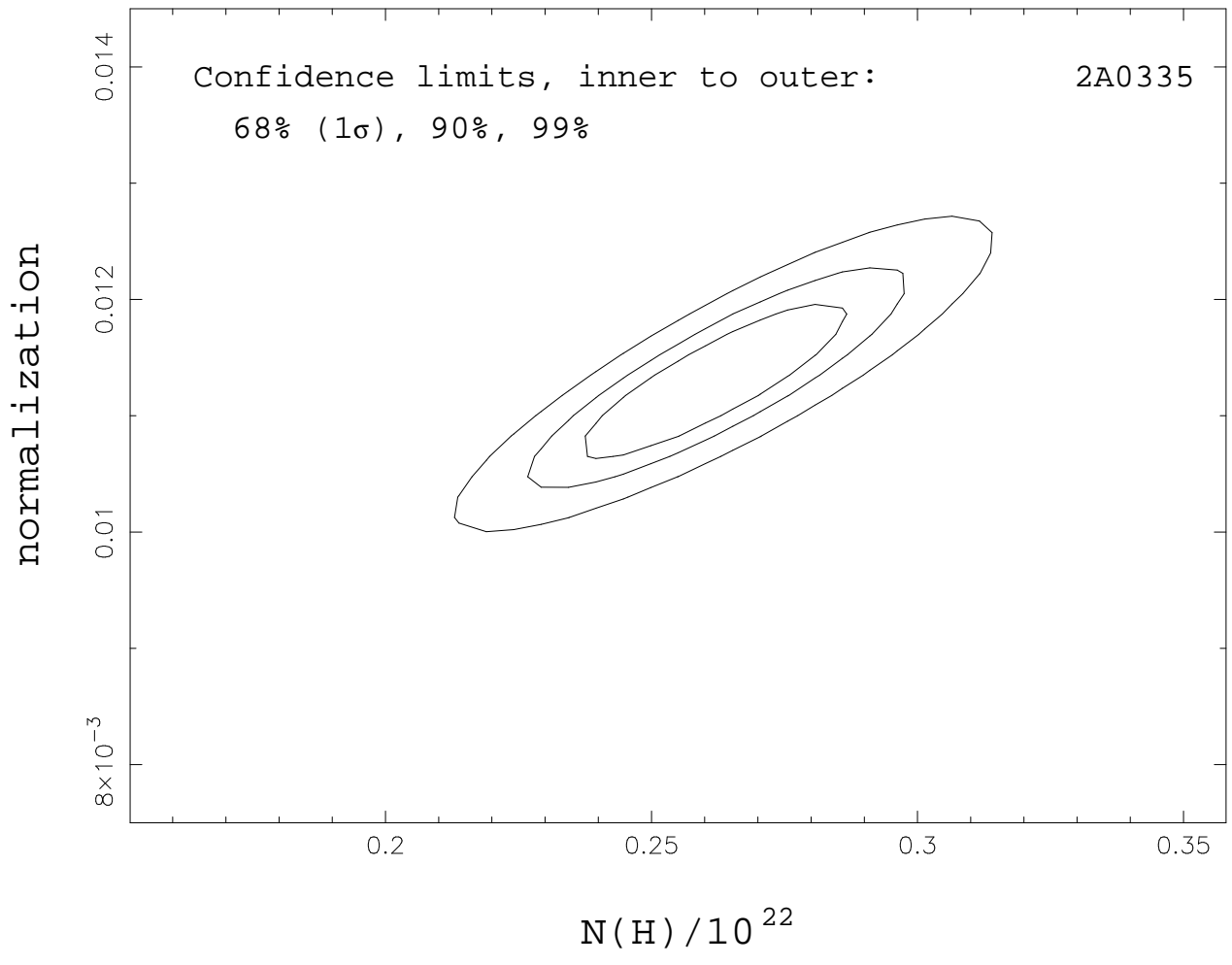
This figure "Fig_IRAS1.jpg" is available in "jpg" format from:

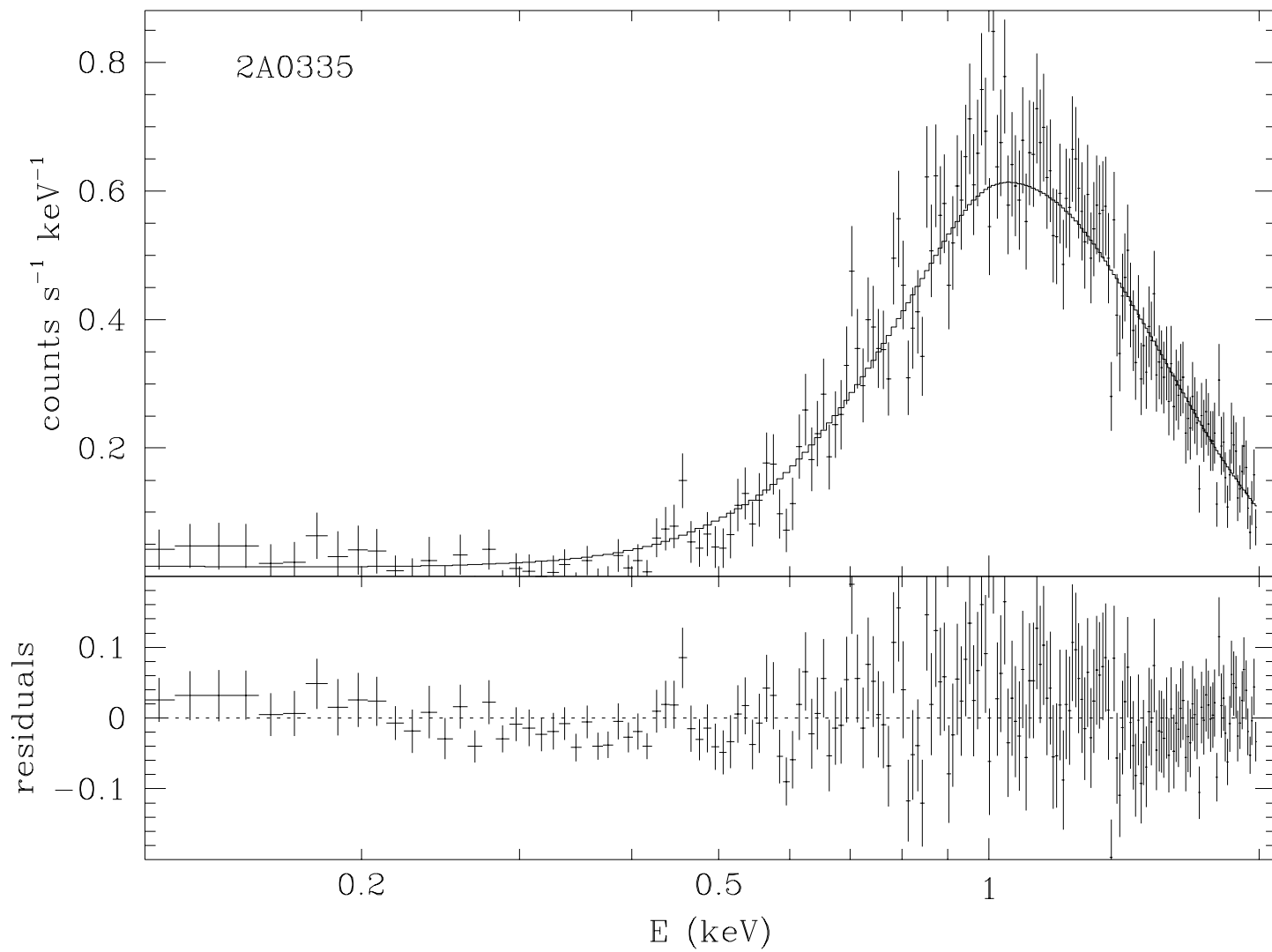
<http://arxiv.org/ps/astro-ph/9806385v1>

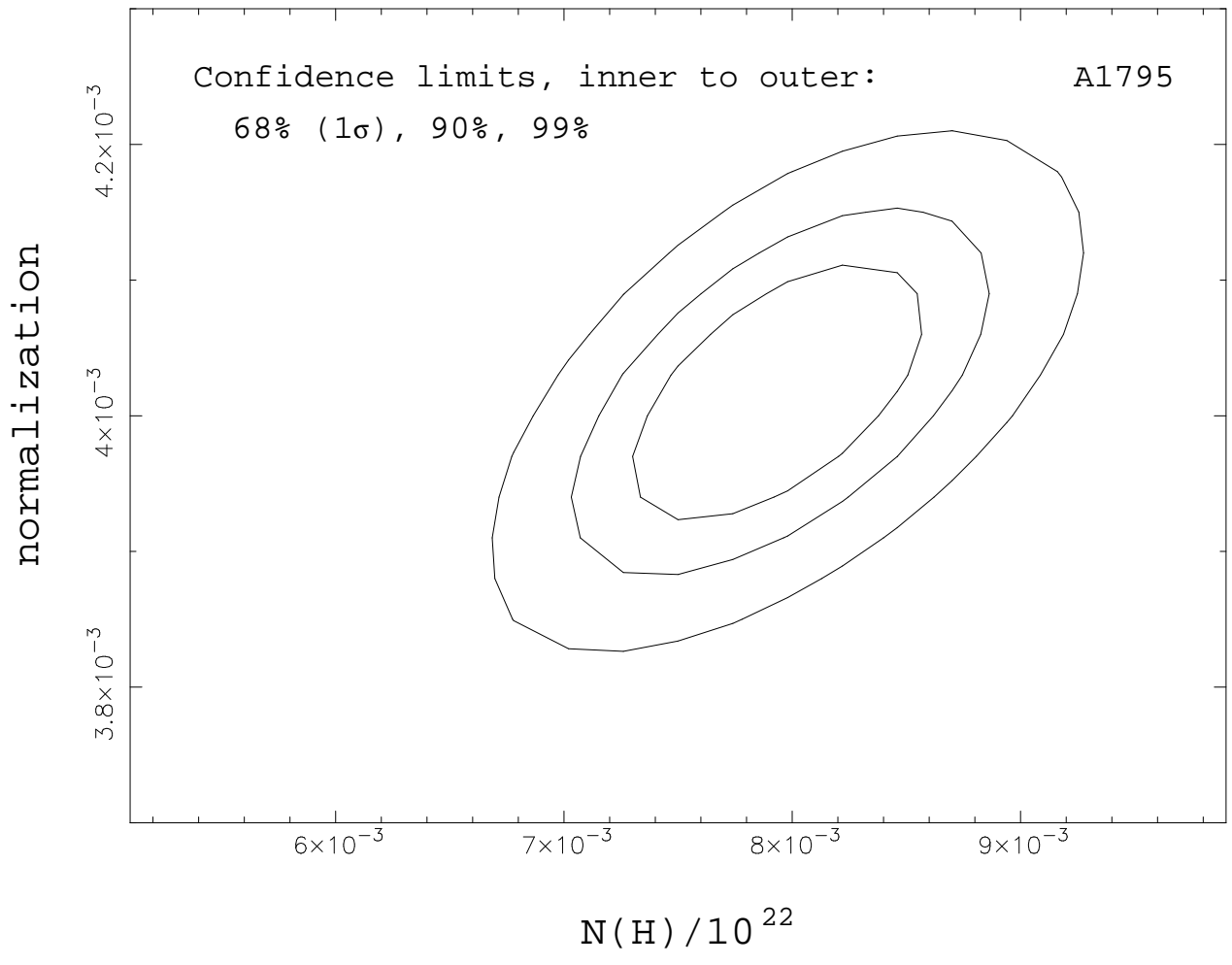


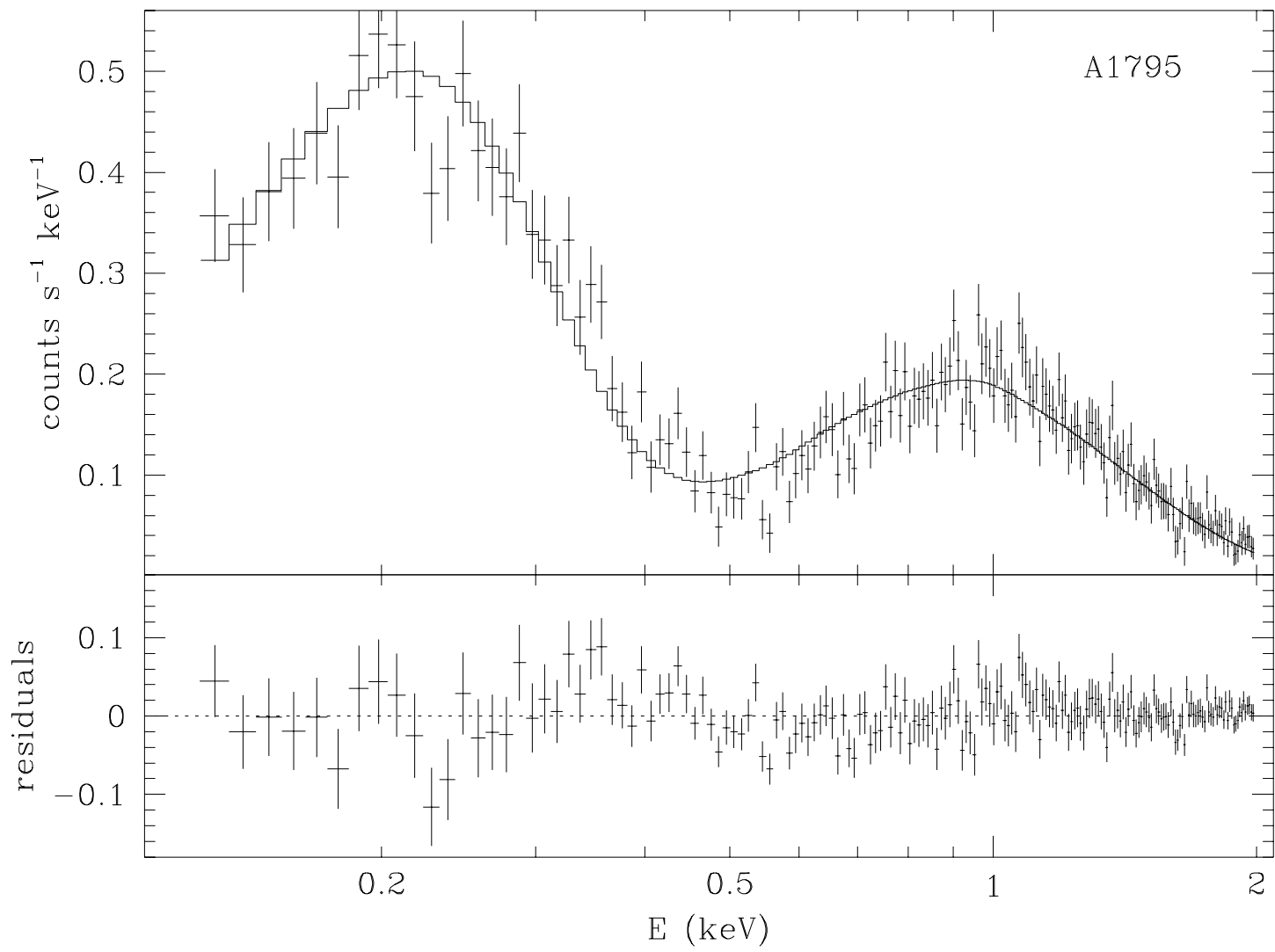
This figure "Fig_IRAS2.jpg" is available in "jpg" format from:

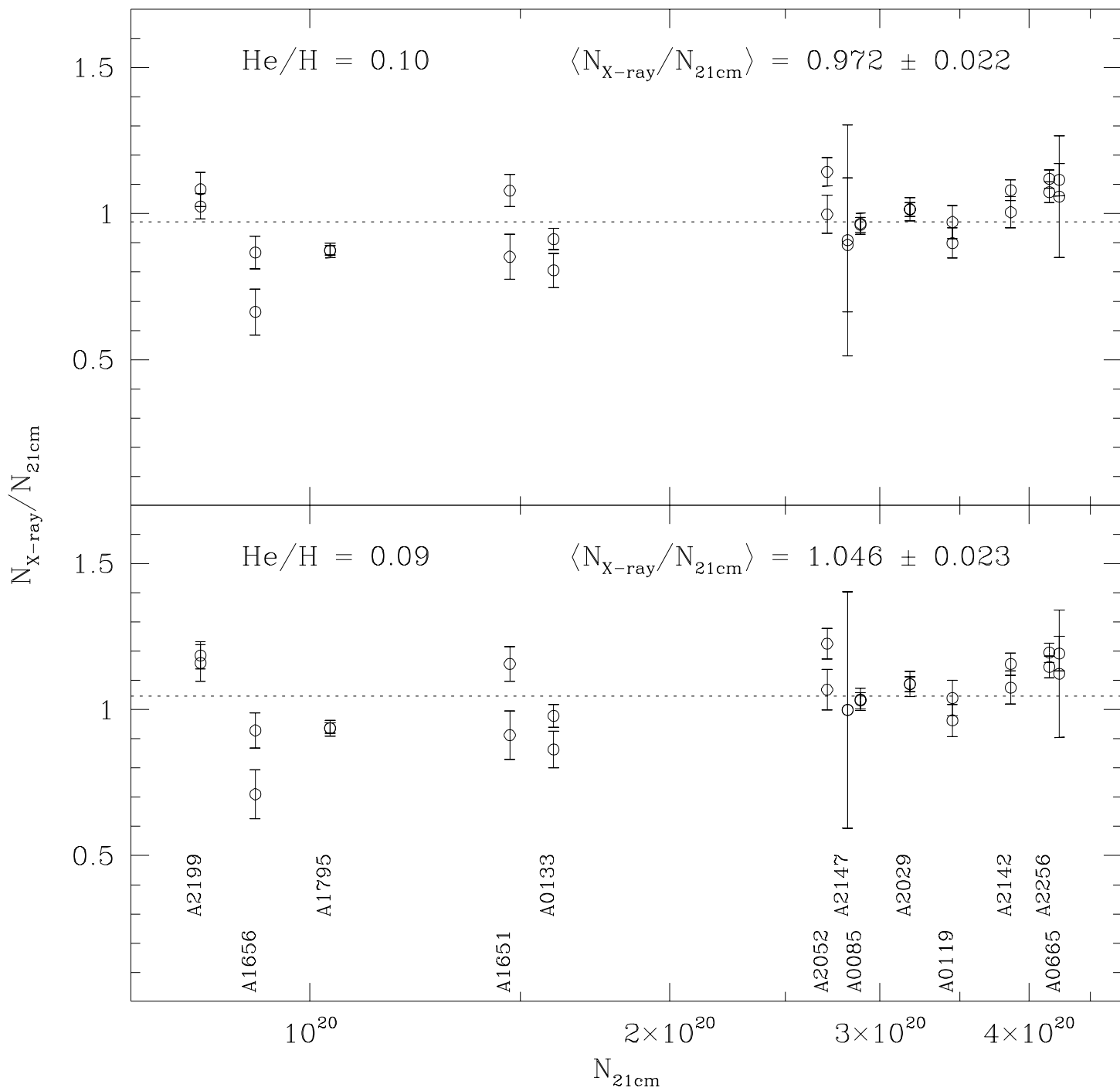
<http://arxiv.org/ps/astro-ph/9806385v1>

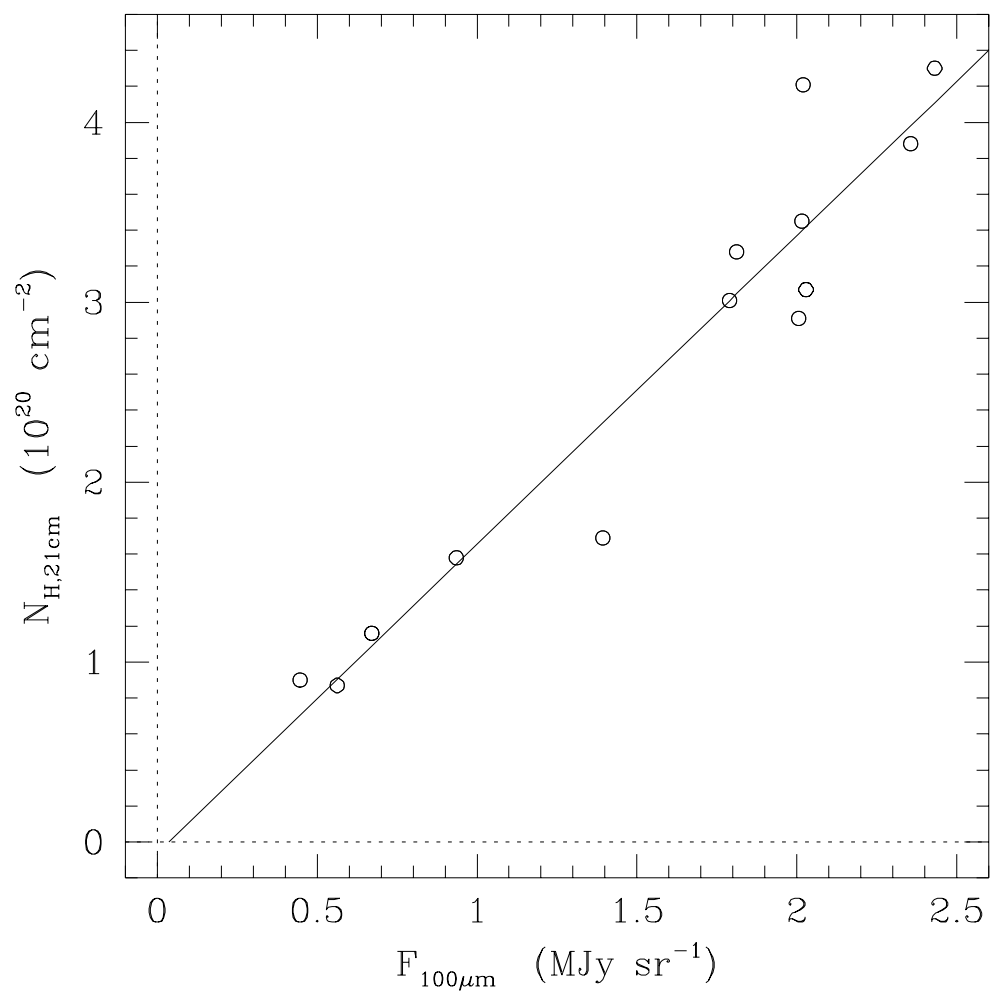


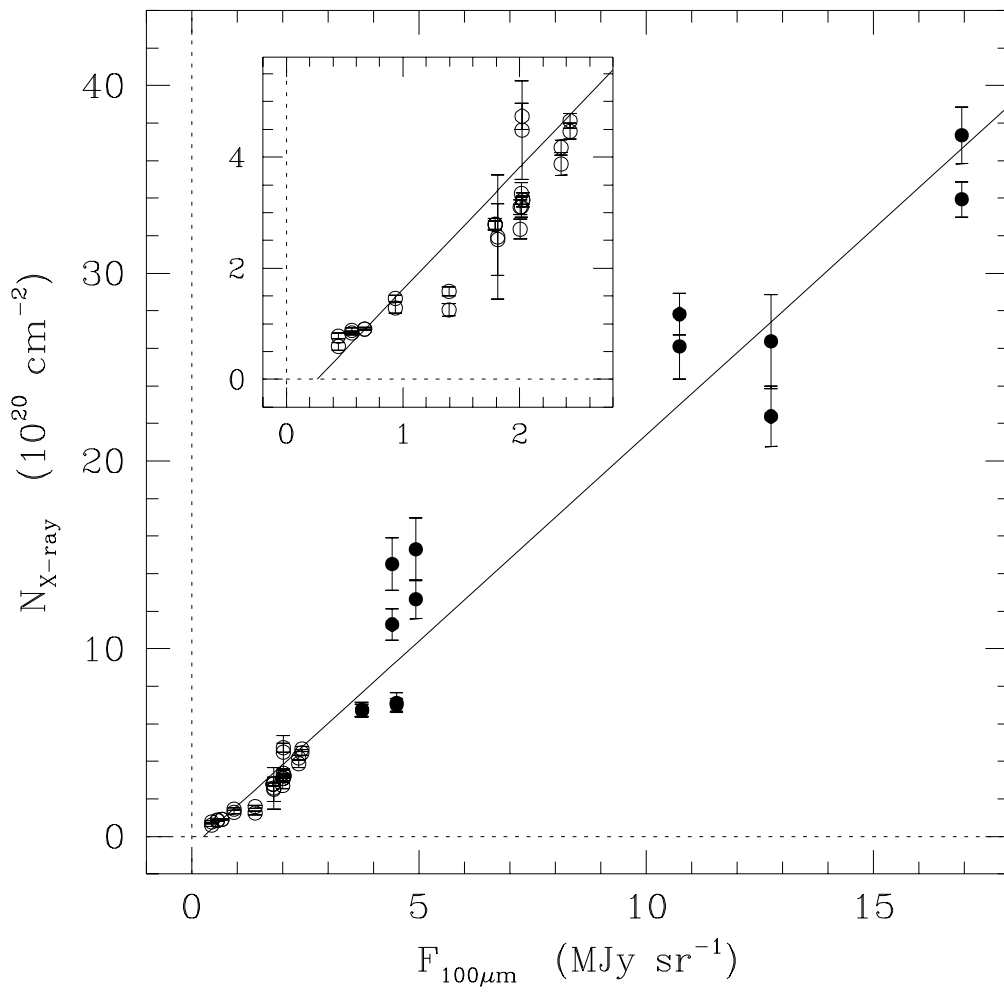


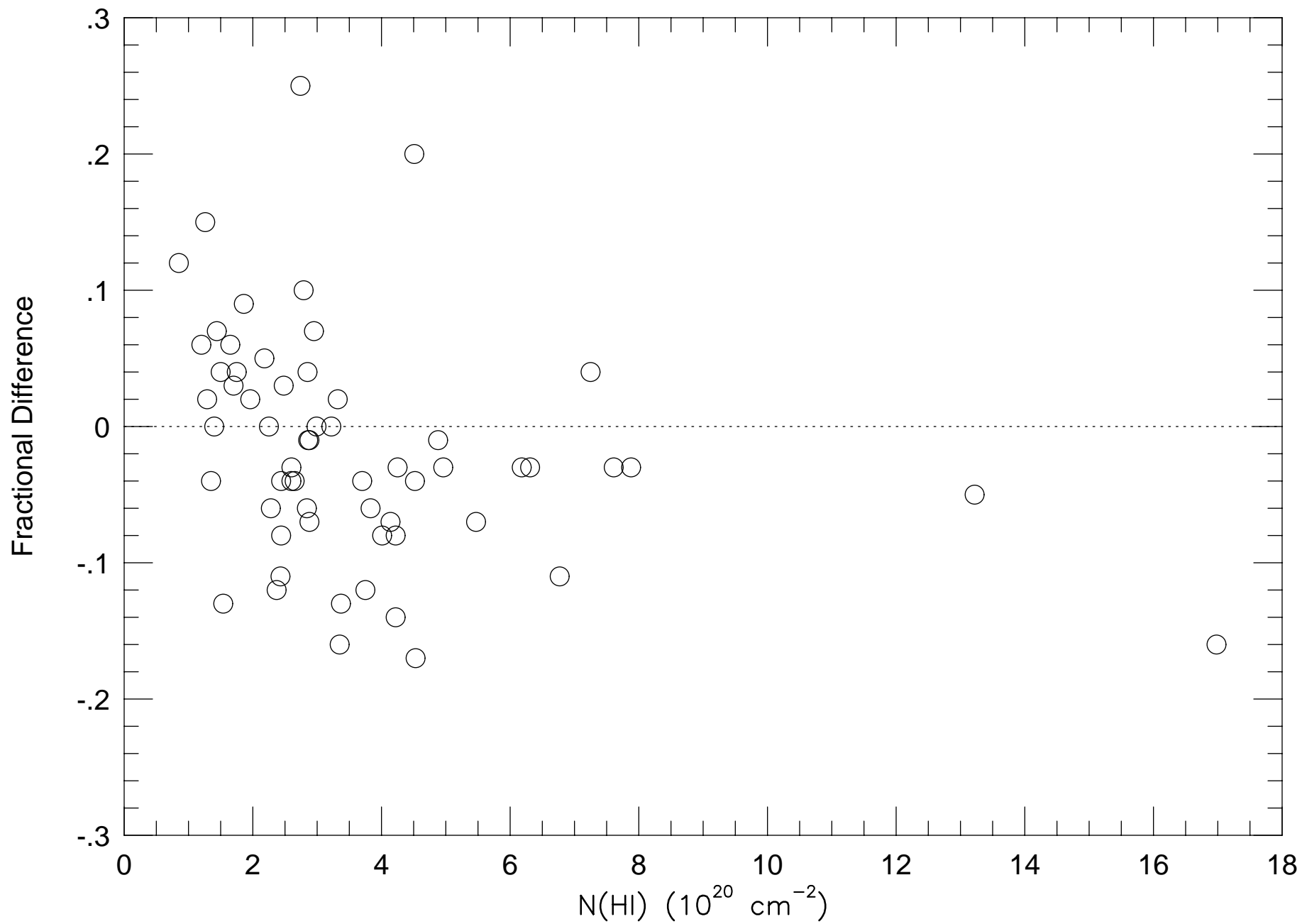






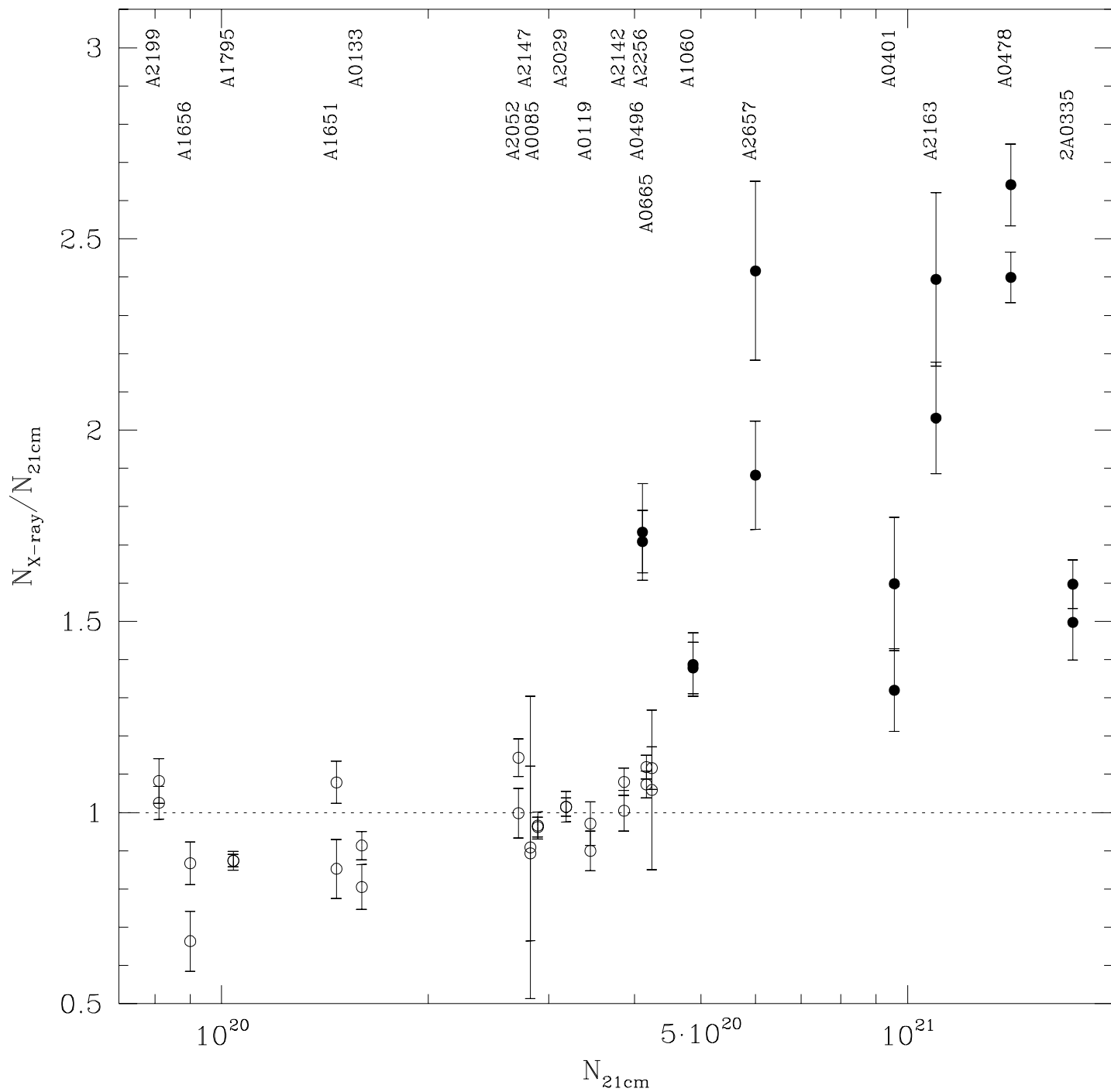






This figure "Fig_NHF100.gif" is available in "gif" format from:

<http://arxiv.org/ps/astro-ph/9806385v1>



This figure "Fig_ann.gif" is available in "gif" format from:

<http://arxiv.org/ps/astro-ph/9806385v1>